Supporting Information

All Fabric-Based Multifunctional Textile Sensor for Detections and Discriminations of Humidity, Temperature, and Strain Stimuli

Shuaitao Yang[1], *Chengwei Li*[1], *Ningxuan Wen*[1], *Shihong Xu*[2], *Hui Huang*[1], *Tianze Cong*[1], *Yongpeng Zhao*[2], *Zeng Fan*[1], *Kun Liu*[3], *Lujun Pan*[*1]

[1]School of Physics, [2]School of Microelectronics and [3]School of Optoelectronic Engineering and Instrumentation Science, Dalian University of Technology, No. 2 Linggong Road, Ganjingzi District, Dalian 116024, P.R. China

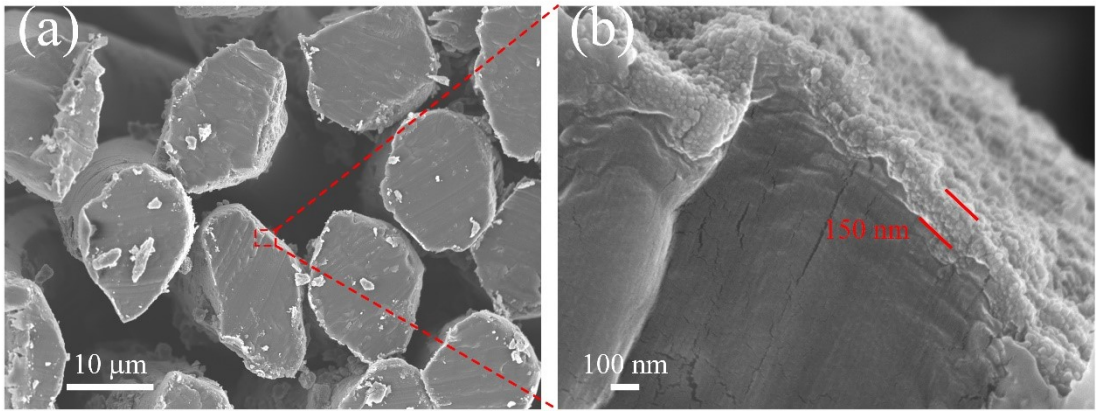

Figure S1. (a) Cross-section images of the carbon particle coated fabric. (b) Enlarged view in (a).

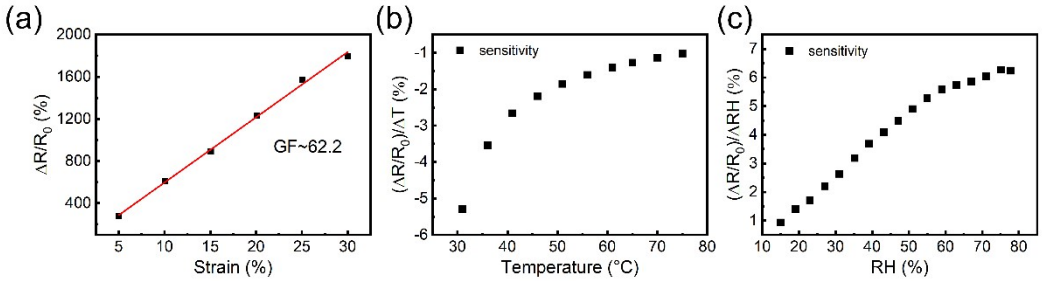

Figure S2. Sensitivity of the conductive fabric in response to (a) strain, (b) humidity, and (c) temperature.

Table S1. Comparison of various textile strain sensors reported in the literature.

Sensing mechanism	Fabrication method	Fabric type	Sensing medium	Gauge factor	Strain range	Ref.
Resistance	Dip-coating	Nylon fabric	Mxene	24.35	0~20%	1
Resistance	Dip-coating	Polyester farbic	RGO	-26 (y direction) -1.7 (x direction)	0~8% 0~15%	2
Resistance	Dip-coating	Cupra fabric	Home-made pen ink	2.63	0~23%	3
Resistance	Dip-coating	Nylon/PU fabric	RGO	18.5 (0~10%) 12.1 (10~18%)	0~30%	4
Resistance	Dip-coating	Nylon/spandex fabric	Carbonic pen ink	62.2	0~30%	This work
Capacitance	Laser cutting	Conductive fabric	Silicone elastomer	1.23	0~100%	5
Capacitance	Multicore-shell printing	Silicone multicore-shell fiber	Ionically conductive fluid	0.35	0~250%	6
Capacitance	Twisting	Ecoflex@CNT core-shell fiber	CNT	0.6	0~200%	7
Capacitance	Sewing	Nylon/spandex fabric	Carbon black	1.5	0~30%	This work

RGO: reduced graphene oxide; Cupra: cuprammonium rayon; PU: polyurethane.

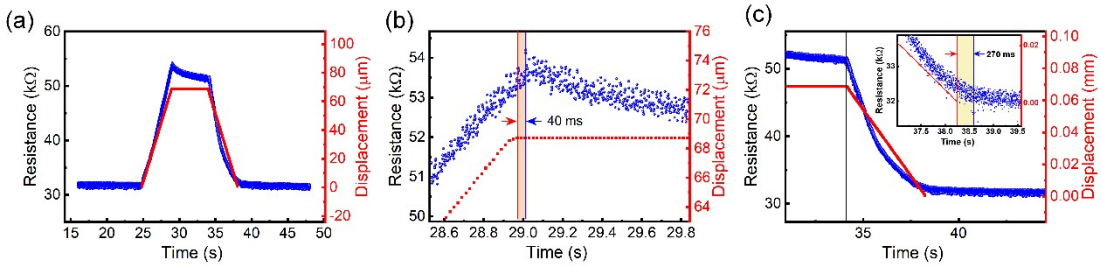

Figure S3. (a) Real-time resistance of the sensor in the process of applying 0-1-0% strain. (b) The delay between the resistive response and the applied strain. (c) Recover time of the sensor in response to 1% strain.

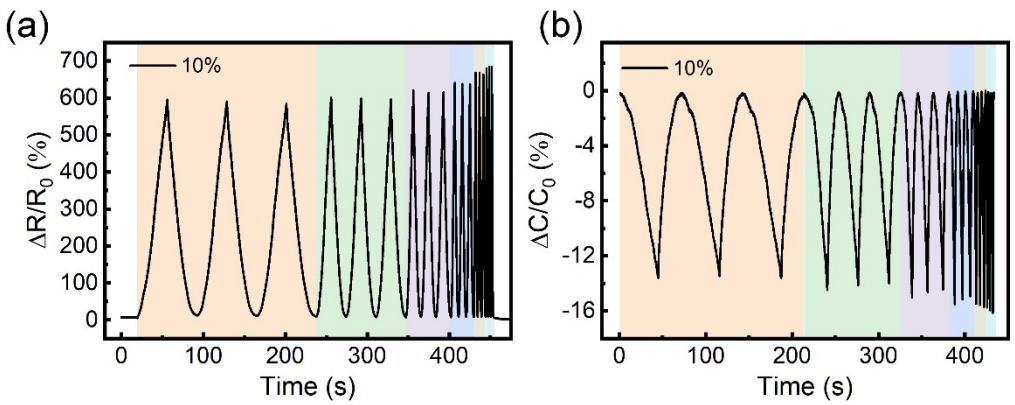

Figure S4. Influence of the strain rate on the sensing properties of (a) resistive and (b) capacitive sensors. The sensor was stretched to 10% at a strain rate of 0.5, 1, 2, 4, 6, 8 mm/min.

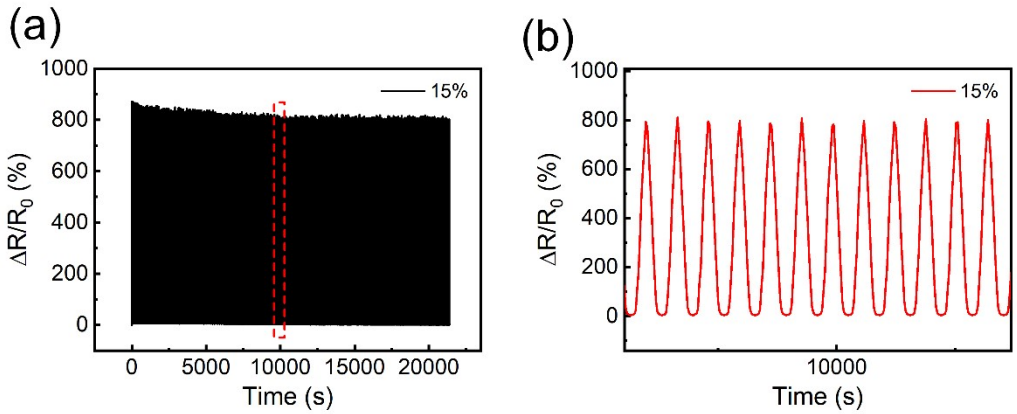

Figure S5. (a) 5000 cycles tensile test of the conductive fabric. (b) Enlarged view of several cycles in (a).

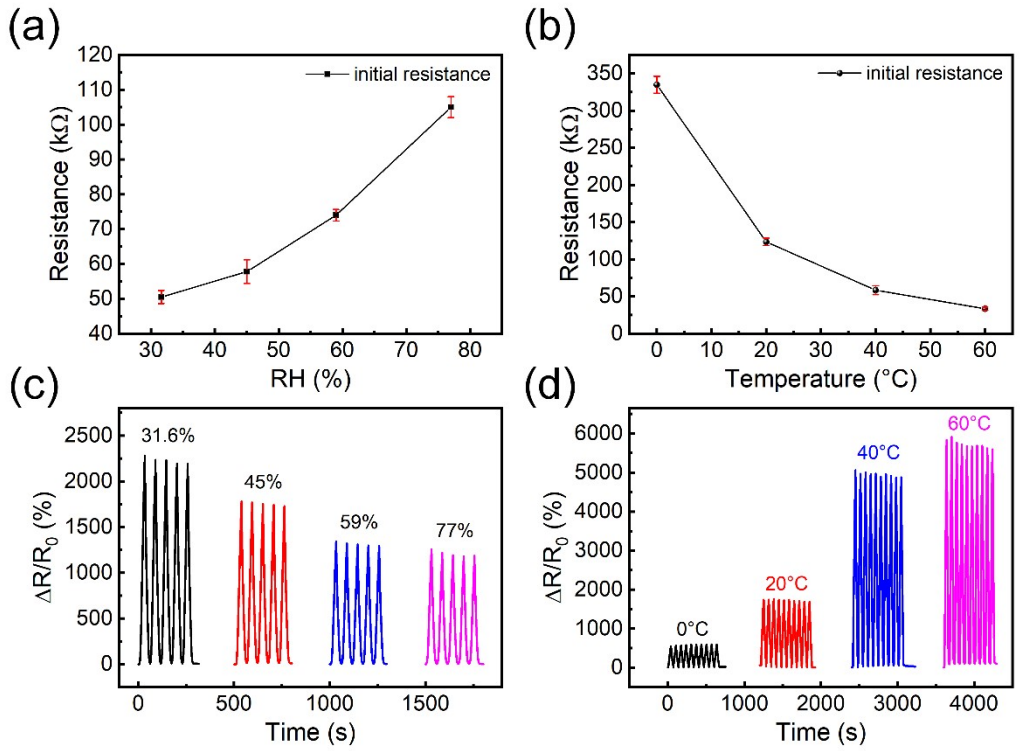

Figure S6. (a) Initial resistance of the conductive fabric at different humidity. (b) Initial resistance of the conductive fabric at different temperatures. Influence of (c) humidity and (d) temperature on strain sensing performance.

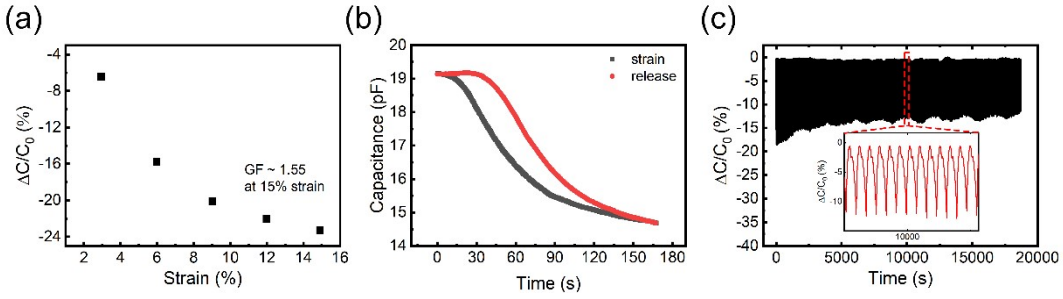

Figure S7. (a) Relative capacitance of the sandwich structured sensor stretched to 15%. (b) Hysteresis behavior of the capacitive strain sensor. (c) Long-term stability test of the capacitance strain sensor in more than 5000 cycles.

Table S2. Initial resistance and capacitance, and sensitivity of the sensors prepared in one batch.

	Sample 1	Sample 2	Sample 3	Sample 4	Sample 5	Mean	S.D.
R_0	38.2 kΩ	33.3 kΩ	34.6 kΩ	31.8 kΩ	34.2 kΩ	34.0	2.55
GF-R	61.5	63.4	65.4	59.2	61.7	62.2	2.31
C_0	15.2 pF	14.5 pF	17.6 pF	14.0 pF	14.8 pF	15.2	1.40
GF-C	1.56	1.43	1.51	1.47	1.50	1.49	0.05

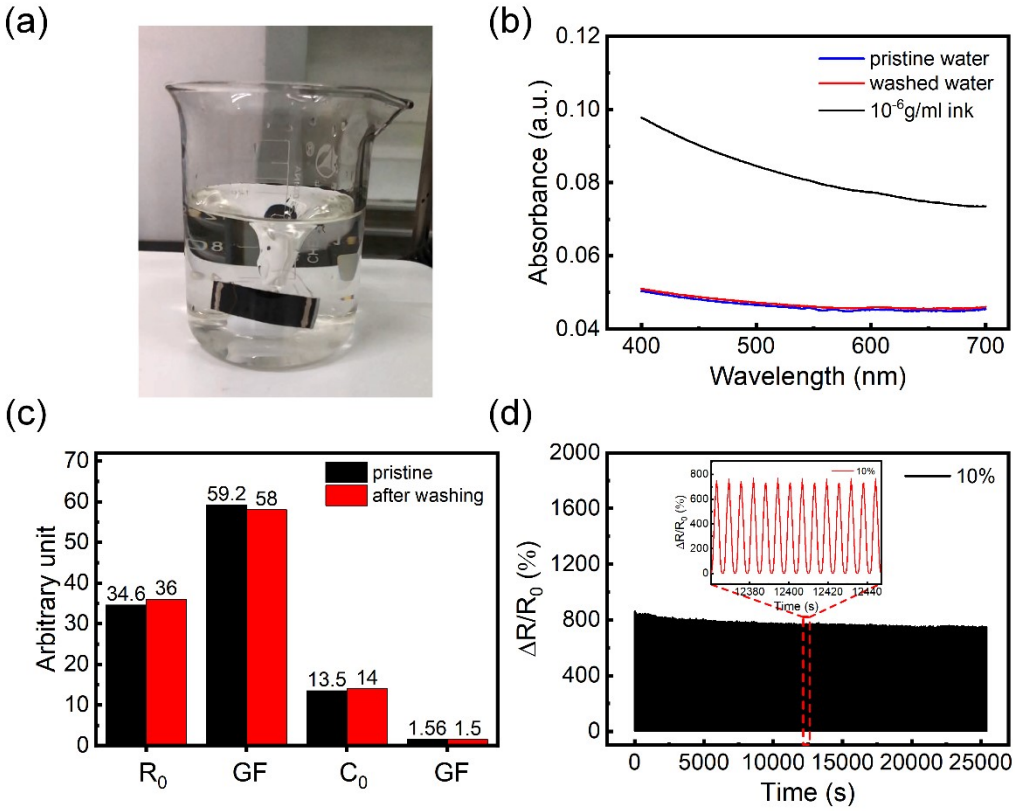

Figure S8. (a) Optical image of the textile sensor washed with water. (b) Visible absorption spectrum of the DI water, washed water, and 10-6 g/ml ink solution. (c) Initial resistance and capacitance, and sensitivity of the corresponding resistive and capacitive sensors. (d) Stability test of the washed textile sensor in more than 5000 cycles.

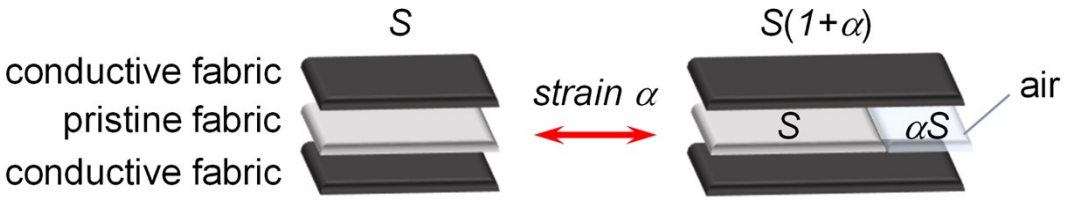

Figure S9. The schematic diagram illustrates the influence of air entry on the capacitance of the sensor during stretching.

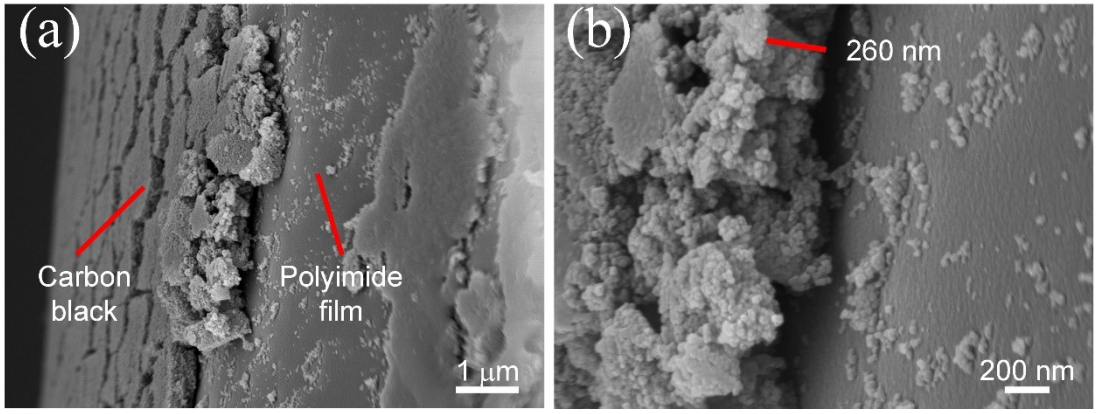

Figure S10. The thickness of the carbon black layer spin-coated on the polyimide film.

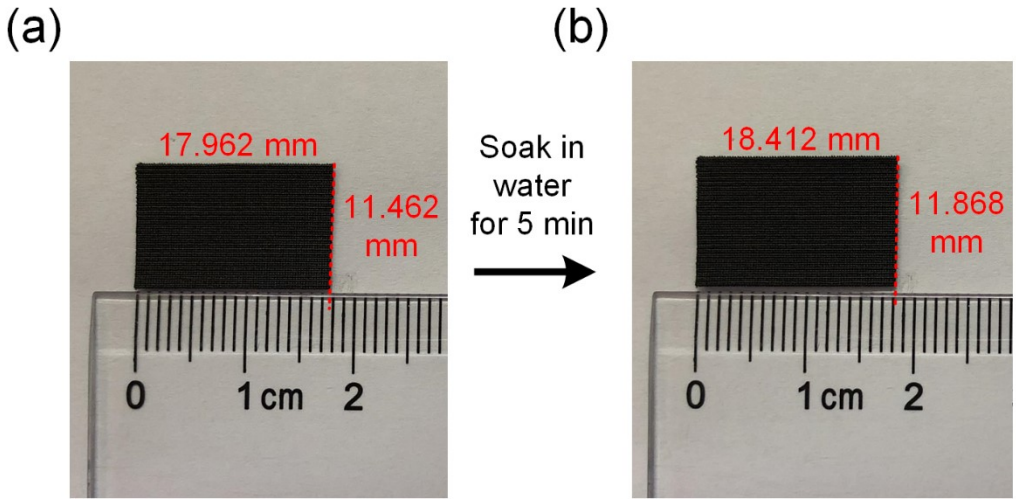

Figure S11. Water swelling of the conductive fabric.

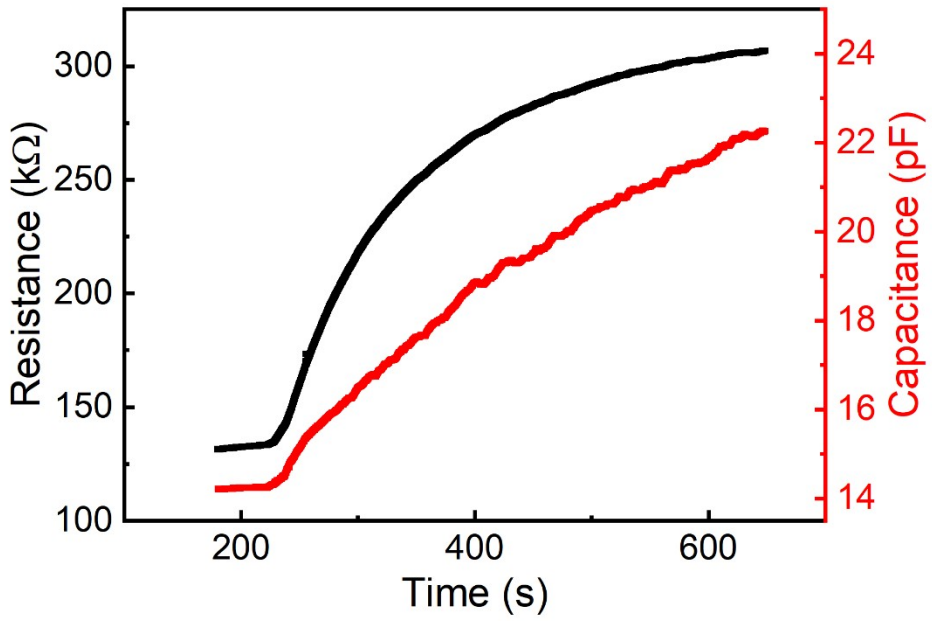

Figure S12. Resistance and capacitance response of the sensor when the baby's diaper gets wet.

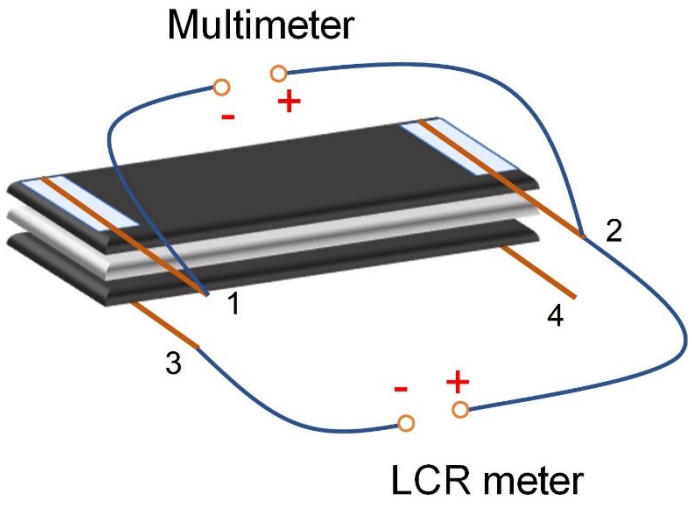

Figure S13. Scheme of measuring resistance and capacitance at the same time.

References

1 L. Yuan, M. Zhang, T. Zhao, T. Li, H. Zhang, L. Chen and J. Zhang, *Sensor Actuat. A Phys.*, 2020, **315**, 112192.

2 Z. Yang, Y. Pang, X.-L. Han, Y. Yang, J. Ling, M. Jian, Y. Zhang, Y. Yang and T.-L. Ren, *ACS Nano*, 2018, **12**, 9134–9141.

3 S. Bi, L. Hou, H. Zhao, L. Zhu and Y. Lu, *J. Mater. Chem. A*, 2018, **6**, 16556–16565.

4 G. Cai, M. Yang, Z. Xu, J. Liu, B. Tang and X. Wang, *Chem. Eng. J.*, 2017, **325**, 396–403.

5 A. Atalay, V. Sanchez, O. Atalay, D. M. Vogt, F. Haufe, R. J. Wood and C. J. Walsh, *Adv. Mater. Technol.*, 2017, **2**, 1700136.

6 A. Frutiger, J. T. Muth, D. M. Vogt, Y. Mengüç, A. Campo, A. D. Valentine, C. J. Walsh and J. A. Lewis, *Adv. Mater.*, 2015, **27**, 2440–2446.

7 C. Choi, J. M. Lee, S. H. Kim, S. J. Kim, J. Di and R. H. Baughman, *Nano Lett*, 2016, **16**, 7677–7684.